An analysis of the clinical significance of the TKI-resistant gene *ZNF687* for hepatocellular carcinoma patients

Guan-Lan Zhang^{1,A,C}, Jian-Di Li^{2,C}, Ji-Feng He^{1,D}, Kun-Jun Wu^{1,B}, Ying-Yu Mo^{1,B}, Song-Yang Zhong^{1,B}, Xuan-Fei Wang^{1,D}, Fei-Fei Wu^{1,D}, Yi-Si Qin^{1,D}, Hong Zhao^{1,D}, Zhi-Guang Huang^{2,E}, Gang Chen^{2,3,E}, Rong-Quan He^{1,3,A,F}

- ¹ Department of Medical Oncology, The First Affiliated Hospital of Guangxi Medical University, Nanning, China
- ² Department of Pathology, The First Affiliated Hospital of Guangxi Medical University, Nanning, China
- ³ Guangxi Key Laboratory of Enhanced Recovery after Surgery for Gastrointestinal Cancer, The First Affiliated Hospital of Guangxi Medical University, Nanning, China
- A research concept and design; B collection and/or assembly of data; C data analysis and interpretation;
- D writing the article; E critical revision of the article; F final approval of the article

Advances in Clinical and Experimental Medicine, ISSN 1899-5276 (print), ISSN 2451-2680 (online)

Adv Clin Exp Med. 2025;34(5):787-801

Address for correspondence

Rong-Quan He E-mail: herongquan@gxmu.edu.cn

Funding sources

The study was financially supported by the following institutions: Guangxi Zhuang Autonomous Region Health Committee Self-financed Scientific Research Project (grant No. Z20201147); Guangxi Medical University Student Innovation and Entrepreneurship Training Program Project (grant No. 202210598057): The First Affiliated Hospital of Guangxi Medical University Provincial and Ministerial Key Laboratory Cultivation Project: Guangxi Laboratory of Enhanced Recovery after Surgery for Gastrointestinal Cancer (grant No. YYZS2020003); Guangxi Medical University Education and Teaching Reform Project (grant No. 2021XJGA02); Guangxi Medical University Teacher Teaching Ability Development Project (grant No. 2202JFA20); Guangxi Higher Education Undergraduate Teaching Reform Project (grants No. 2022JGA146 and No. 2021JGA142); and Guangxi Educational Science Planning Key Project (grant No. 2022ZJY2791).

Conflict of interest

None declared

Received on November 14, 2023 Reviewed on January 29, 2024 Accepted on May 8, 2024

Published online on October 2, 2024

Cite as

Zhang GL, Li J-D, He J-F, et al. An analysis of the clinical significance of the TKI-resistant gene *ZNF687* for hepatocellular carcinoma patients. *Adv Clin Exp Med*. 2025;34(5):787–801. doi:10.17219/acem/188425

D0

10.17219/acem/188425

Copyright

Copyright by Author(s)
This is an article distributed under the terms of the
Creative Commons Attribution 3.0 Unported (CC BY 3.0)
(https://creativecommons.org/licenses/by/3.0/)

Abstract

Background. Novel treatments such as monotherapy and combined immunotherapy significantly extend overall survival (OS) for hepatocellular carcinoma (HCC) patients, but HCC is susceptible to treatment resistance during long-term therapy. The resistance mechanism to targeted drugs in HCC remains ambiguous, making research on HCC drug resistance targets crucial for the development of precision medicine.

Objectives. To investigate the transcriptional features, biological functions and potential clinical value of the tyrosine kinase inhibitor (TKI)-resistant gene *ZNF687* in HCC.

Materials and methods. The TKI-resistant genes of HCC were identified using clustered regularly interspaced short palindromic repeats (CRISPR) in vitro screening. Then, the dependence of HCC cell lines on *ZNF687* was investigated in silico. We collected global mRNA datasets of HCC tissue, integrated the mRNA expression characteristics of *ZNF687* in HCC and explored the impact of *ZNF687* on HCC patient prognoses using the Kaplan—Meier method (in silico). The Gene Ontology (GO) and Kyoto Encyclopedia of Genes and Genomes (KEGG) pathways analyses were then conducted, and a connectivity map and molecular docking technology were applied to find the underlying agent opposing ZNF687.

Results. In vitro, the guide RNA corresponding to *ZNF687* was weakly detected in HCC cells, and *ZNF687* deficiency was found to inhibit growth in HCC cell lines. *ZNF687* mRNA was overexpressed and had a high discriminatory ability for HCC in 2,975 HCC samples, contrasting with 2,340 non-HCC samples. Moreover, an excessive *ZNF687* transcript level was related to a worse overall survival (OS) prognosis. Histone modification, spliceosome, transcription coregulator activity, and nucleocytoplasmic transport were the most significant pathways for *ZNF687* differential-related gene enrichment. Chaetocin was found to be a candidate compound and presented a strong affinity to ZNF687.

Conclusions. *ZNF687* represents a TKI-resistant and growth-dependent gene for HCC, the overexpression of which indicates poor OS for HCC patients. Additionally, ZNF687 is expected to be a druggable target for overcoming TKI resistance, and chaetocin may be a candidate therapeutic compound for ZNF687.

Key words: tyrosine kinase inhibitor, resistance, mRNA, hepatocellular carcinoma, ZNF687

Background

According to statistics from the American Cancer Society (ACC), the mortality rate of liver cancer has fallen compared to previous decades. However, the burden of liver cancer is still heavy, with the estimated number of deaths ranking 5th among all cancer deaths in men and 7th in women.¹ Generally, hepatocellular carcinoma (HCC) dominates liver cancer cases (75-85%),2 and the risk factors include hepatitis virus infection, alcohol and aflatoxin, as well as water contamination.^{3,4} A lack of specific clinical signs in the early stages of HCC causes many diagnoses to be delayed until an advanced stage. With early diagnosis, liver transplantation and surgical resection are the recommended therapy choices. Because the complete resection of pathological tissue is difficult, patients are at risk of tumor recurrence, metastasis, hemorrhage, infection, and abdominal wall hernia.5,6 Advanced HCC is common in clinical practice and has a poor prognosis for many complications, such as serious ascites, jaundice, hemorrhage, and hepatic encephalopathy. For instance, the prognosis of advanced HCC combined with obstructive jaundice is poor, and although endoscopic biliary drainage may improve patient outcomes, the risk of cholangitis increases.^{7,8} Currently, systematic therapy, especially tyrosine kinase inhibitors (TKI), is suggested for advanced HCC patients who are classed as A class using Child-Pugh score for hepatic function. Due to the disorder of protein kinase activity in many malignancies, targeting protein kinases has become a significant anti-cancer strategy. Tyrosine kinase inhibitor is one of the U.S. Food and Drug Administration (FDA)-approved protein kinase inhibitors, which occupy an important position in targeted therapy.¹⁰ Monotherapy or combined immunotherapy significantly extends HCC patients' survival times. Nevertheless, HCC is susceptible to treatment resistance during long-term medication therapy,11 leading to relapse and disease progression.¹² The problem is that TKI resistance occurs in the late stage of treatment, which limits long-term therapeutic benefits.¹³ Regrettably, the resistance mechanisms of targeted drugs in HCC have not been completely elucidated except for epithelial-mesenchymal transition, ATP-binding cassette transporters, hypoxia, autophagy, and angiogenesis. 14 Therefore, research on the mechanism and therapeutic target of HCC drug resistance is crucial for improving treatment response, reducing complications, and thus enhancing long-term efficacy.

Clustered regularly interspaced short palindromic repeats (CRISPR)/CRISPR-associated (Cas) is an RNA-guided and Cas nuclease-cleaved gene-editing technique that can modify a single gene and reveal its function. ^{15,16} There are 3 groups of CRISPR/Cas systems, with CRISPR/Cas9 belonging to the 2nd category. ¹⁷ CRISPR/Cas9 comprises the Cas9 nuclease and CRISPR RNA or gRNA, which can lead Cas9 to specific sites and cut DNA for gene knockout. ¹⁸ Genome-wide CRISPR knockout screening

(GeCKO) technology offers an effective method for observing genomic alterations under certain conditions. During the CRISPR loss-of-function screen, gRNAs are randomly carried into various cells by lentiviral vectors containing Cas9 and puromycin resistance. Cells that are not effectively transfected by the lentivirus are eliminated by puromycin, and a collection of genome-wide mutant HCC cells is created. The genomic expression profile of mutant cells changes under a particular intervention, and high-throughput sequencing is utilized to detect variations between treatment and control groups. In this work, we conducted an in vitro CRISPR screen experiment for TKI resistance in HCC cells and gathered genes instead of TKIs. *ZNF687* was identified as a TKI-resistant gene and is anticipated to be a therapeutic target for HCC.

Located at chromosome 1q21.3,²¹ ZNF687 is a recently discovered C₂H₂-type zinc finger protein that has been reported to be overexpressed in the kidneys, spleen and other hemopoietic organs and to be associated with the proliferation and differentiation of hematopoietic cells.²² Aberrant *ZNF687* expression is a driver of some cancers. For instance, ZNF687 mutations are implicated in Paget's disease of bone, and their overexpression is linked to giant cell tumors associated with Paget's disease of bone. 21,23,24 It is now suspected that ZNF687 may induce HCC cells to produce stem cell-like characteristics by upregulating BMI1, NANOG and OCT4, which then contributes to HCC progression. In vitro experiments have demonstrated that ZNF687 knockdown increases the susceptibility of HCC cells to cisplatin; thus, ZNF687 may be engaged in the development of HCC chemoresistance.²² However, no studies have discovered the mechanism of ZNF687 that results in tumor-targeted drug resistance.

Consequently, this is the first comprehensive research to explore the expression status, TKI therapy response, biology, and clinical implications of *ZNF687* in HCC. We hypothesized that *ZNF687* may be a candidate gene for TKI resistance in HCC, estimated the mean expression level of the *ZNF687* gene using global HCC cohorts, and analyzed its capacity to distinguish HCC tissue from controls. Survival curves and clinicopathological characteristics analysis were applied to investigate the association between *ZNF687* transcriptional-level expression and patient prognosis. Moreover, we identified the potential molecular mechanism and predicted the underlying therapeutic component based on the biological abnormalities resulting from increased *ZNF687* expression.

Objectives

This study was designed to investigate the transcriptional expression features, biological functions and potential clinical value of the TKI-resistant gene *ZNF687* in HCC, exploring the probability of overcoming the TKI-resistance problem.

Materials and methods

In vitro genome-wide CRISPR/Cas9 knockout library

Experimental material

The experiment followed the protocol described in the research of Joung et al.²⁵ The human HCC cell line Huh7 was acquired from the cell bank of the Chinese Academy of Sciences (Beijing, China). The genome-wide CRISPR knockout v2 (GeCKO v2) library and gRNA were obtained from the Addgene Corporation (Watertown, USA; https://www.addgene.org/pooled-library/zhang-human-gecko-v2; 1000000048).

Lentivirus transfection

When cell growth reached 70–90% confluence, the adherent cells were separated with trypsin and counted. In total, 1.10×10^8 cells were transfected with the GeCKO v2 library containing 65,386 specific gRNAs. The multiplicity of infection was controlled to be <0.3.

TKI intervention and DNA extraction

Hepatocellular carcinoma cells successfully infected with lentivirus were dosed with the TKI drug for 21 days. The TKI component we adopted, anlotinib, was sourced from the Jiangsu Zheng Da Tian Qing company (Nanjing, China). Afterward, we used a Quick-DNA Midiprep Plus Kit (D4075) developed by Zymo Research (Orange, USA) to extract the DNA of the surviving HCC cells for library construction and high-throughput sequencing.

Library construction

The library construction was completed by the Beijing Nuo He Zhi Yuan Technology Company (Beijing, China), according to the following process. The extracted DNA was randomly digested into 350 bp fragments using a Covaris breaker (Covaris, Woburn, USA). The library was then prepared after conducting terminal repair and adding a poly-A-tail, and index connectors sequentially to the DNA fragments.

Analysis of sequencing results and negative screening strategies

Two treated samples and 2 control samples were subjected to high-throughput sequencing by the Beijing Nuo He Zhi Yuan Technology Company. After connector data, unknown data and low-quality test data were removed and quality control was conducted using FastQC software, high-quality gene counts were included. Model-based

analysis of genome-wide CRISPR/Cas9 knockout software was employed for positive and negative screening. Both analysis tools were employed with default parameters, and genes corresponding to significantly reduced gRNAs were considered potential TKI-resistant genes.¹⁹

Gene effect

The gene effect can reflect the necessity of a specific gene in various cell lines. We downloaded the data for "CRISPR (DepMap 22Q2 Public + Score Chronos)" from the Cancer Dependency Map website (DepMap; https://depmap.org/portal/). The "gene effect" values of each cancer cell line after *ZNF687* knockout or inhibition were extracted, and a scatterplot was drawn using the ggplot2 package. The effects of *ZNF687* deficiency on the growth vitality of 20 HCC cell lines were then investigated.

Collection strategy of mRNA datasets

Microarray and RNA sequencing datasets were retrieved and screened from multiple databases, including the Gene Expression Omnibus (GEO) (https://www.ncbi. nlm.nih.gov/geo/), ArrayExpress (https://www.ebi.ac.uk/ arrayexpress/), Oncomine (https://www.oncomine.com/), The Cancer Genome Atlas (TCGA) (https://portal.gdc. cancer.gov/), and Genotype-Tissue Expression (https:// www.gtexportal.org/) on March 1, 2023, using the following search terms: (malignancy OR cancer OR tumor OR neoplasia OR carcinoma OR carcinomatosis) AND (hepatocellular OR liver OR hepatic OR HCC). The datasets were included if they met the following criteria, namely: 1) the species was homo sapiens; 2) there were tissue samples; and 3) there were at least n = 3 HCC and noncancerous tissue samples. Simultaneously, samples that had been genetically modified or treated with drugs were excluded. The screened data were then further processed, and datasets from the same platform were merged and eliminated using batch effect, and unstandardized datasets were normalized with the $log_2(x + 1)$ method.

Combined analysis in silico

We integrated the 35 public datasets and computed the standardized mean difference (SMD) to compare the *ZNF687* mRNA expression differences between HCC tissue and noncancerous tissue. For each dataset, the sample number, average expression level and standard deviation (SD) of *ZNF687* in HCC tissue and noncancerous tissue were listed. The I² index and Q test were used to examine the overall heterogeneity of the data, with I² > 50% or p < 0.10 illustrating obvious heterogeneity, for which the random-effect model was chosen. Otherwise, the fixed-effect model was used to combine the SMDs. To appraise the differential diagnostic significance of *ZNF687* for HCC, a summary receiver operating characteristic (SROC) curve

was created. Sensitivity, specificity and likelihood ratios were used to assess the effectiveness of the diagnostic test, and publication bias was detected using the Egger's test.

Prognostic analysis in silico

The clinicopathological information of 333 HCC patients was downloaded from TCGA, and the clinical value of ZNF687 mRNA expression levels on HCC patient outcomes was investigated using univariate Cox regression with clinicopathological features. A Schoenfeld residual was analyzed for proportional hazards (PH) assumption, and a Martingale residual was analyzed to detect whether the log-hazard function was linearly related to the continuous variable ZNF687 expression. McFadden's pseudo-R² was employed to determine the goodnes-of-fit, with a Mc-Fadden's pseudo-R² closer to 1 indicating better goodness-of-fit. During data cleaning, clinical parameters with more uncertain information (e.g., "Unknown," "unreport," "Tx," "Nx," and "Mx") were eliminated. For the identification of overall survival (OS), if a patient's survival status was "alive", the survival time was selected as the last follow-up time. In the event that a patient's survival status was "dead", the OS was selected as the time of death. Finally, the impact of each clinicopathological parameter on HCC patient outcomes was assessed by independently calculating the hazard ratios (HRs) of ZNF687 expression, age, sex, race, primary T (pT) stage, and American Joint Committee on Cancer (AJCC) stage. Additionally, the survminer R package was utilized to identify the optimum cutoff value, which divided the 333 samples into a high-expression ZNF687 group and a low-expression ZNF687 group, and the relationship between ZNF687 mRNA status and HCC patient prognosis was explored through the Kaplan-Meier method. The computational formula was as follows:

> McFadden's R² = = [(likelihood (null) – likelihood (model))/ /likelihood (null)]

Biological pathway exploration

An expression profile of 371 HCC tissue samples and 50 control samples (data source: TCGA) was executed using the limma package in R 4.1.1 (R Foundation for Statistical Computing, Vienna, Austria). The genes with a log fold change (logFC) of >1 were defined as differentially high expression genes of HCC. Genes with a strongly positive relationship to *ZNF687* (Pearson's correlation coefficient >0.75) were acquired using Pearson's analysis. ²⁶ *ZNF687*-related differential genes were obtained by intersecting differential highly expressed genes and *ZNF687* strongly positively correlated genes, which were used for enrichment analysis of the Gene Ontology (GO) and Kyoto Encyclopedia of Genes and Genomes (KEGG) pathways. The STRING tool v. 11.5 (https://cn.string-db.

org/) was employed to calculate the connection score between *ZNF687*-related differential genes, and the potential protein complex subnetworks were analyzed using the molecular complex detection (MCODE) algorithm with Cytoscape software (https://cytoscape.org).

Candidate drugs prediction and evaluation in silico

A connectivity map (CMAP) is a query tool for predicting candidate drugs by comparing similarities or dissimilarities between the reference perturbation signatures and the input gene set.²⁷ In this study, due to the limitation of no more than 150 genes in the CMAP tool for drug prediction, the ZNF687 genes positively related (Pearson's coefficient >0.80) and simultaneously differentially upregulated in HCC were inputted to CMAP (https://clue. io/query) to predict the compounds opposing ZNF687. The two-dimensional (2D) structure of each molecular drug was downloaded from the PubChem database (https://pubchem.ncbi.nlm.nih.gov/), and energy was minimized via Chem3D software (PerkinElmer Informatics, Inc, Waltham, USA). The AlphaFold structure of ZNF687 (ID: Q8N1G0) was downloaded from the UniProt database (https://www.uniprot.org/). Subsequently, PYMOL 2.5.2 (https://pymol.org) and Autodock Vina 1.1.2 (https:// autodock.scripps.edu) were used to simulate the docking of each candidate compound, and the molecular structure of ZNF687.²⁸ Discovery Studio v. 4.5 software (https:// www.3ds.com/products/biovia/discovery-studio) was used to visualize the docking results.

Statistical analyses

R 4.1.1, Stata v. 17 (StataCorp LLC., College Station, USA) and IBM SPSS v. 26 (IBM Corp., Armonk, USA) were used for statistical analyses. Standardized mean difference was calculated as an effect indicator to reveal the mRNA expression status of ZNF687 in HCC tissue. The I² index and Q test were used to examine the overall heterogeneity of the data, and sensitivity analysis and meta-regression analysis were used to explore the sources of heterogeneity. The summary receiver operating characteristic (SROC) curve, sensitivity, specificity, and positive and negative likelihood ratios were analyzed to evaluate the discrimination efficiency of ZNF687 for HCC. For the area under the SROC curve (AUC), the criteria for verifying its efficacy were as follows: 0.50-0.70 indicated low estimated capacity, 0.70-0.80 indicated moderate estimated capacity, 0.80-0.90 indicated good, estimated capacity, and an AUC > 0.90 indicated strong estimated capacity. The Egger's test was utilized for detecting publication bias. The univariate Cox regression and Kaplan-Meier methods were applied to explore the prognostic risk factors. The analysis was considered statistically significant at a value of p < 0.05.

Results

CRISPR positive and negative screening in vitro

Under the positive and negative screening results (Fig. 1), 904 lowly enriched gRNAs (logFC < 0) and 949 gRNAs highly enriched gRNAs (logFC > 0) were identified (ttest with a p < 0.05). Compared with the control group, gRNA corresponding to $\it ZNF687$ was weakly detected in the whole-genome mutant HCC cells treated with TKI (logFC = -0.56, t-test with a p = 0.048), which suggested that for $\it ZNF687$ -defective HCC cells, they were more sensitive to TKI intervention and more likely to die.

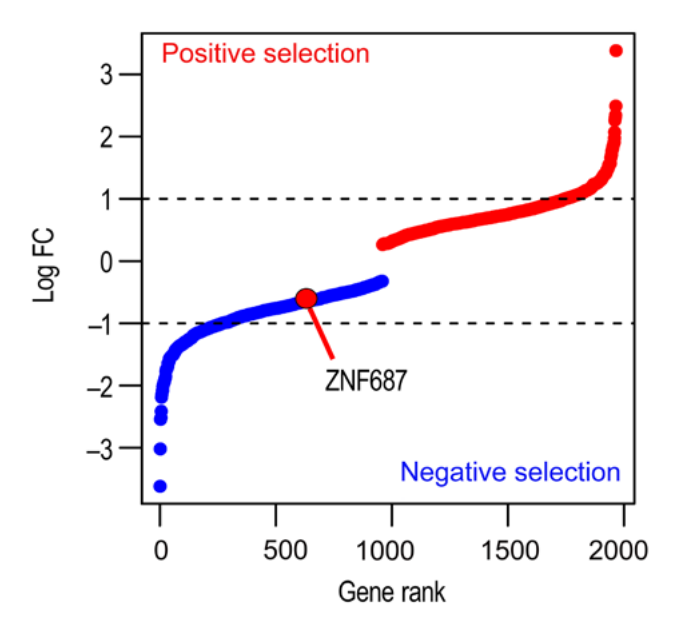


Fig. 1. Positive and negative selections of the clustered regularly interspaced short palindromic repeats screening experiment

Gene rank: The order of all genes after ranking according to the logFC value. The genes with logFC <0 were considered the potential resistant genes, and the genes with logFC >0 were considered the potential sensitive genes.

Carcinogenic effect of ZNF687

The gene effect of *ZNF687* was less than 0 in 19 HCC cell lines (SNU182, PLCPRF5, JHH2, JHH4, JHH6, SNU387, HLF, SKHEP1, SNU423, JHH5, SNU761, SNU398, JHH7, SNU475, JHH1, HUH7, SNU886, HUH1, and SNU449) and greater than 0 only in the HEPG2 cell line (Fig. 2, Supplementary Table 1). Thus, the high expression of *ZNF687* likely promoted HCC cell growth.

Overexpression of ZNF687 and its discriminatory efficacy against HCC

In total, 35 mRNA datasets were collected (Fig. 3), including 2,975 HCC tissue samples and 2,340 noncancerous tissue samples. The ZNF687 transcriptional expression in each dataset, displayed as mean and SD, is shown in Supplementary

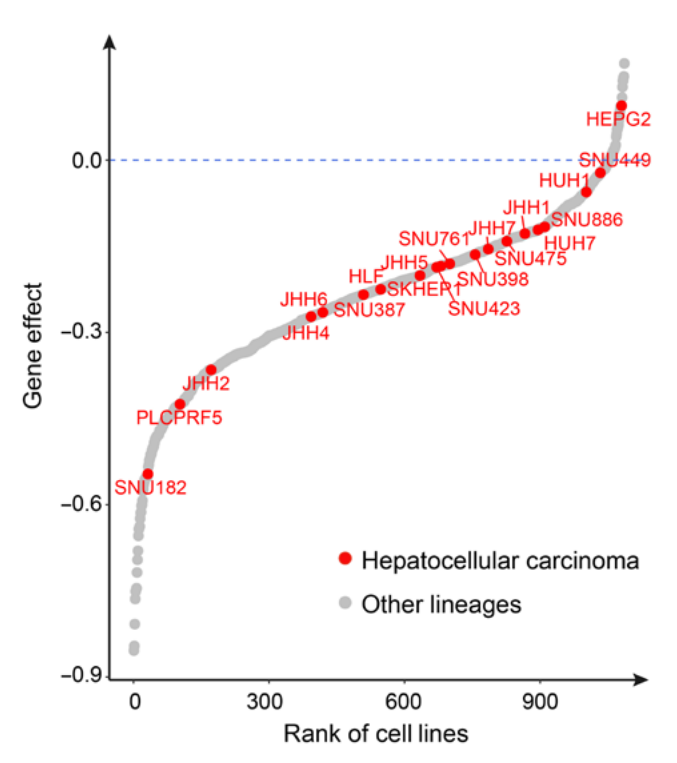


Fig. 2. The zinc finger protein 687 gene dependency distribution for 20 cell lines of hepatocellular carcinoma

Rank of cell lines: The order of all cell lines after ranking according to the gene effect scores. A score <0 indicates cell inhibition after knocking out the gene.

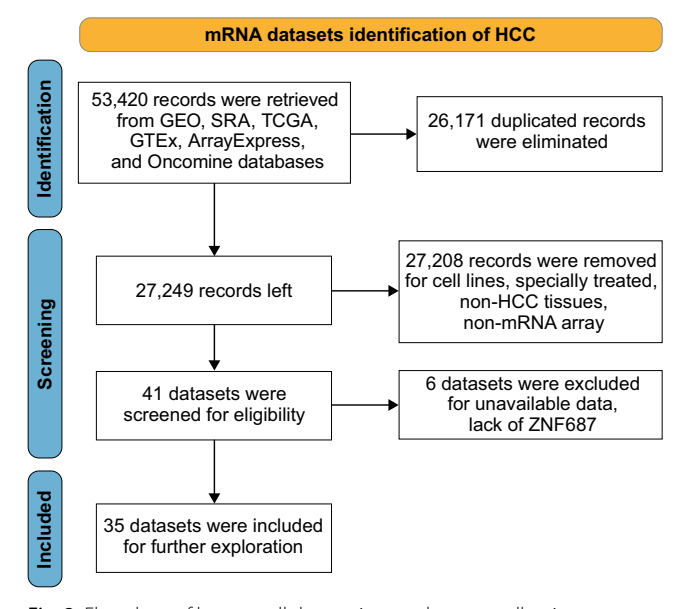


Fig. 3. Flowchart of hepatocellular carcinoma datasets collection

Table 2. The SMD was greater than 0 in most separate datasets, and the combined SMD was 1.10 (95% confidence interval (95% CI): 0.87–1.33), indicating that *ZNF687* was upregulated at the transcriptional level in large HCC samples (Fig. 4A). The results of the $\rm I^2$ index and Q test suggested high heterogeneity ($\rm I^2$ = 90.4%, Q test with a p < 0.01), so the random-effect model was applied. For the investigation of heterogeneity, sensitivity analysis indicated that

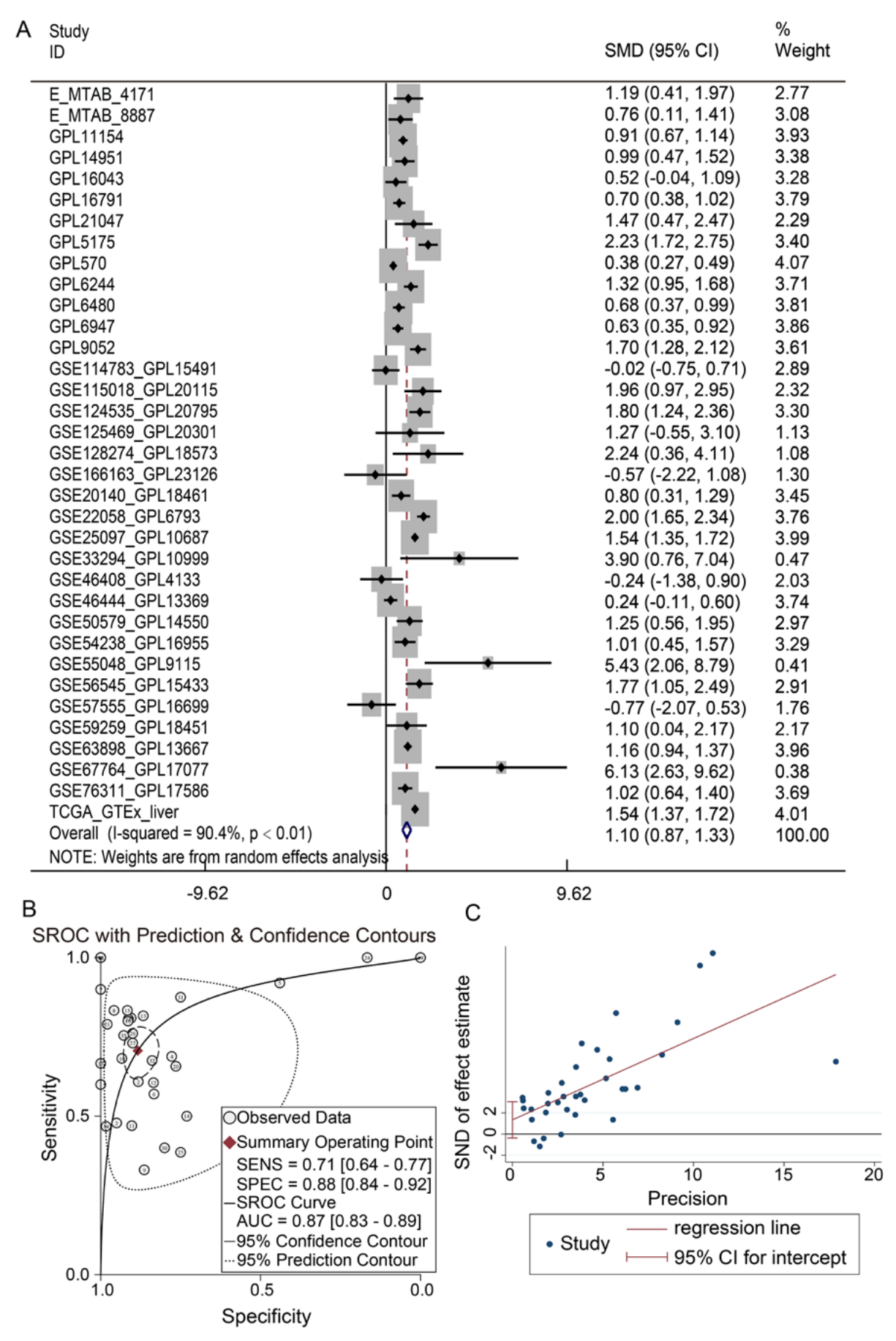


Fig. 4. mRNA expression status of zinc finger protein 687 in hepatocellular carcinoma tissue. A. Forest map of the standardized mean difference; B. Summary receiver operating characteristic (ROC) curve; C. Egger funnel plot (p = 0.12)

Adv Clin Exp Med. 2025;34(5):787-801

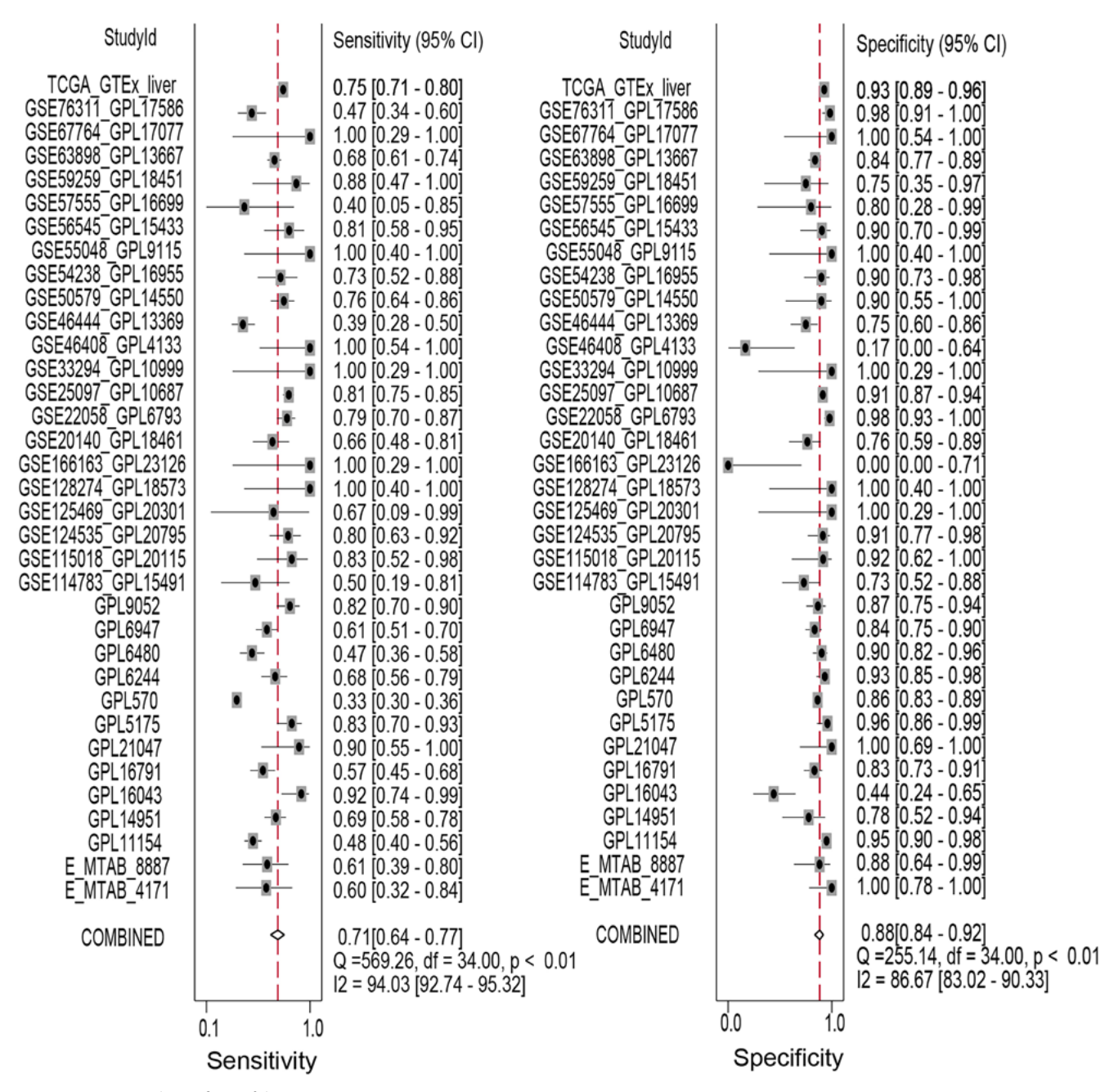


Fig. 5. Sensitivity and specificity of diagnostic test

the pooled SMD was greater than 0 and stable after removing any of the datasets (Supplementary Fig. 1). Based on the result of the meta-regression analysis, the sequencing technique contributed to the heterogeneity (p < 0.01), but neither the merged datasets nor the sample size demonstrated any relationship to the heterogeneity (Supplementary Table 3). The AUC was 0.87 (95% CI: 0.83–0.89) (Fig. 4B), the sensitivity was 0.71 (95% CI: 0.64–0.77) (Fig. 4B, Fig. 5) and the specificity was 0.88 (95% CI: 0.84–0.89) (Fig. 4B, Fig. 5). The positive and negative likelihood ratios were respectively 6.09 (95% CI: 4.25–8.71) (Fig. 6) and 0.33 (95% CI: 0.27–0.41) (Fig. 6), indicating a high discrimination capacity of ZNF687 for HCC. Finally, no compelling publication bias was found according to the Egger's test (p = 0.12) (Fig. 4C).

Clinical significance

Based on the Kaplan–Meier curves, OS time appeared more depressed in the ZNF687-overexpression group (288 samples) than in the ZNF687 underexpression group (45 samples), with an HR of 2.00 (95% CI: 1.09–3.69, logrank test with a p < 0.05) (Fig. 7). This illustrates that elevated mRNA expression of ZNF687 may be connected with poor prognosis in HCC. According to the Supplementary Fig. 2, the Schoenfeld residuals of "ZNF687 (continuous)," "Age," "Gender," "pT stage," and "AJCC stage" show no relationship with time and comply with the PH assumption (PH test, p > 0.05), but the covariate "Race" does not comply with the PH assumption (PH test, p < 0.05). The predictor

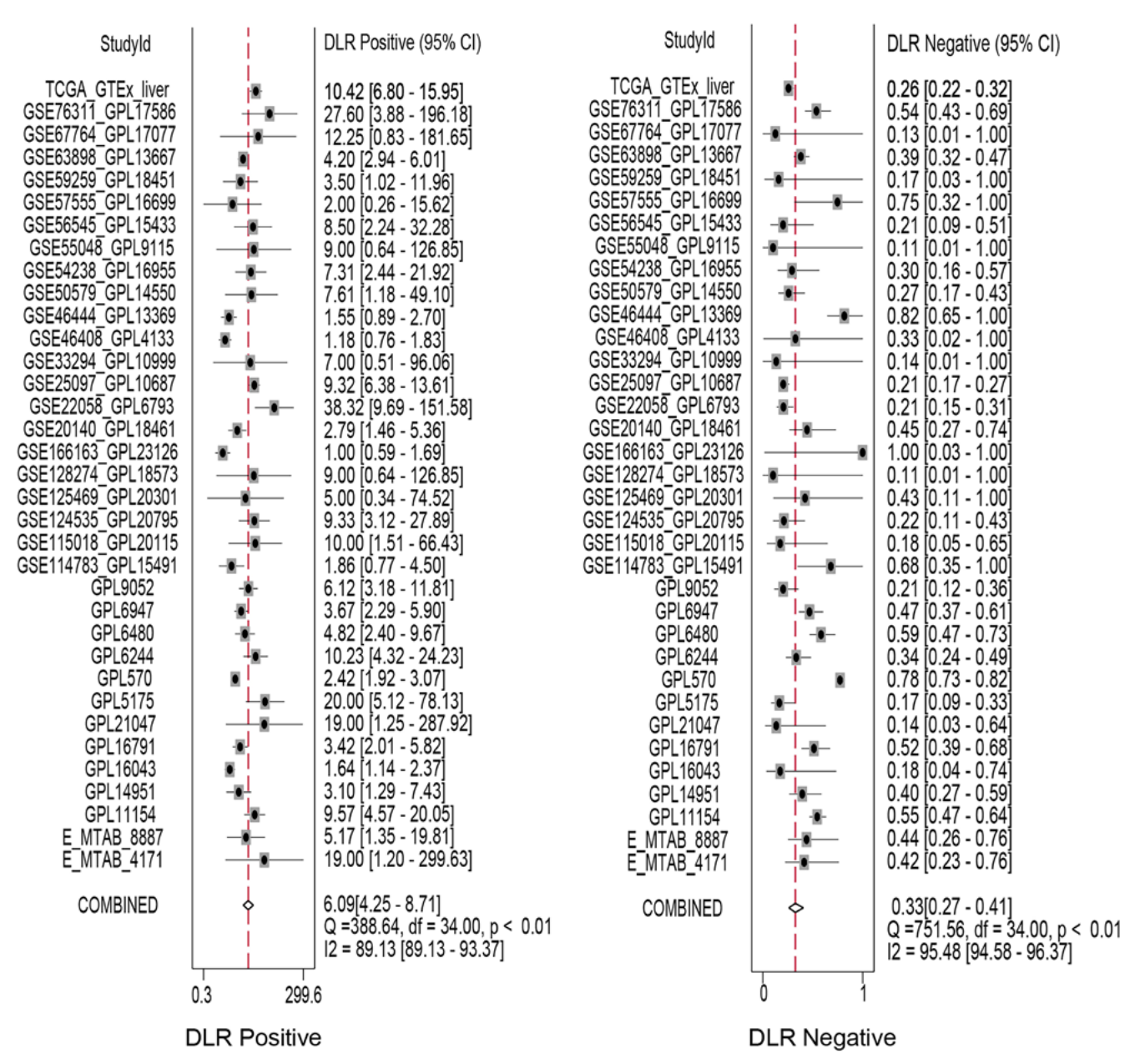


Fig. 6. Double likelihood ratios of a diagnostic test

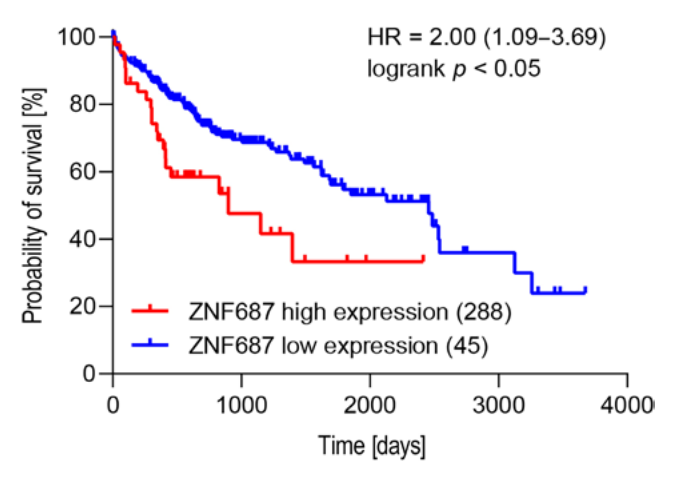


Fig. 7. Association between zinc finger protein 687 transcriptional level and the overall survival (OS) prognosis of hepatocellular carcinoma (hazard ratio (HR) = 2.00, 95% confidence interval (95% CI): 1.09–3.69, logrank test with a p < 0.05)

Table 1. Clinicopathologic features associated with hepatocellular carcinoma death using univariate Cox analysis

Variables	HR (95% CI)	Wald test p-value	McFadden's pseudo R²
ZNF687 (continuous)	1.01 (1.00–1.02)	0.04	<0.01
Age (>65 vs ≤65 years)	1.14 (0.78–1.67)	0.49	<0.01
Gender (male vs female)	0.76 (0.52–1.12)	0.17	<0.01
Race (Asian vs non-Asian)	_	_	_
T (T3 + T4 vs T1 + T2) pT stage (pT3+pT4 vs pT1+pT2)	2.47 (1.68–3.61)	<0.01	0.02
AJCC stage (stage III+IV vs stage I+II)	2.45 (1.67–3.58)	<0.01	0.02

HR – hazard ratio; 95% CI – 95% confidence interval; AJCC – American Joint Committee on Cancer...

Adv Clin Exp Med. 2025;34(5):787-801

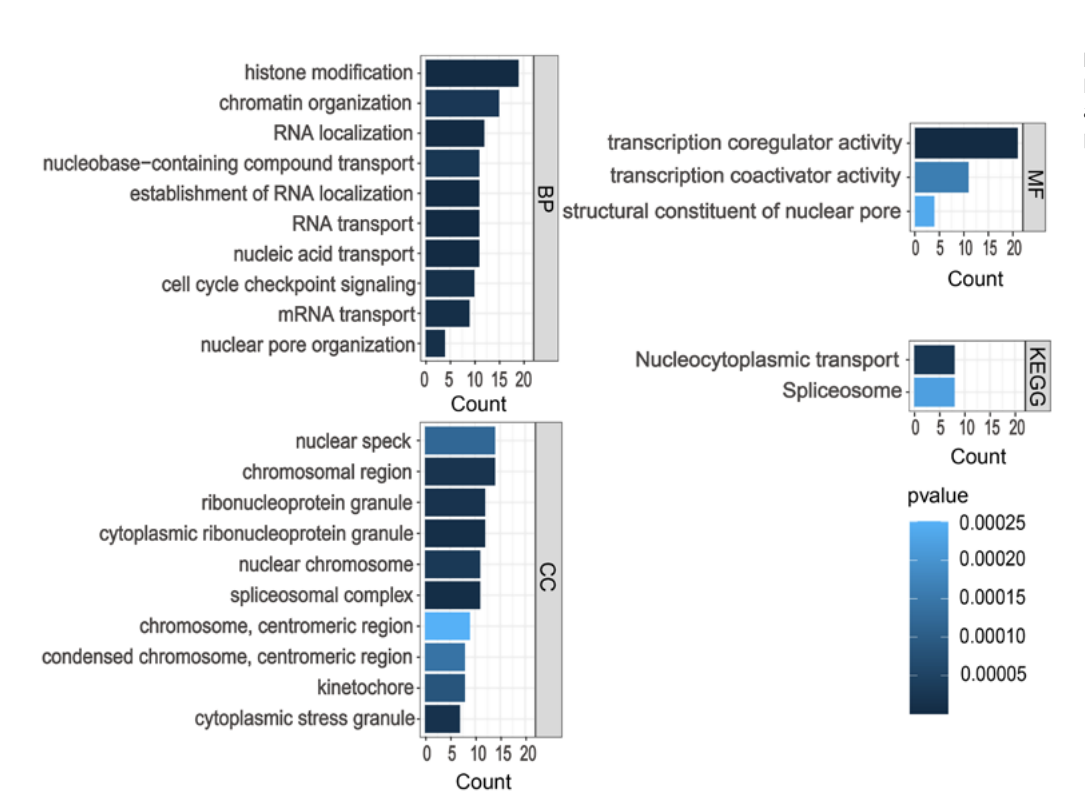


Fig. 8. Gene Ontology (GO) and Kyoto Encyclopedia of Genes and Genomes (KEGG) functional pathways

ZNF687 (continuous) shows no linearity to the log hazard (Supplementary Fig. 3). In line with univariate Cox analysis (Table 1), individuals with a high *ZNF687* expression level had a higher risk of HCC death (HR = 1.01, 95% CI: 1.00-1.02, Wald test with a p = 0.04, McFadden's pseudo $R^2 < 0.01$). The probability of death in "T3 + T4" and "III + IV" HCC patients was higher than that in "T1 + T2" and "I + II" patients, with HRs of 2.47 (95% CI: 1.68-3.61, Wald test with a p < 0.01, McFadden's pseudo $R^2 = 0.02$) and 2.45 (95% CI: 1.67-3.58, Wald test with a p < 0.01, McFadden's pseudo $R^2 = 0.02$), respectively. Age and gender were not statistically significant regarding the HCC outcome (Wald test with a p > 0.05, McFadden's pseudo $R^2 < 0.01$).

GO and KEGG functional pathways

We intersected 2,705 differentially expressed HCC genes and 401 strongly positive *ZNF687*-related genes, of which 214 *ZNF687*-related differential genes were obtained and considered to have an oncogenic effect in HCC cooperating with *ZNF687*. The GO analysis showed that the 214 *ZNF687*-related differentially expressed genes were significantly enriched for "histone modification" of the biological process (BP) and "nuclear speak" of the cellular component (CC), and had "transcription coregulator activity" of molecular function (MF). For the KEGG pathway analysis, "nucleocytoplasmic transport" and "spliceosome" predominated (Fig. 8). Six protein-protein interaction networks were listed through the MCODE algorithm (Table 2). The GO-BP analysis was performed on the network with the highest score, and it was noted that the gene within

Table 2. Protein-protein interaction network analysis based on the MCODE algorithm

Cluster	Score	Nodes	Edges	Node IDs
1	9.333	10	42	ILF2, PTBP1, NONO, RBMX, PSME3, U2AF2, HNRNPU, ILF3, CPSF6, CHTOP
2	6.75	17	54	NUP205, MSH2, MCM2, PARP1, NUP133, MDC1, AHCTF1, TIMELESS, XPO1, CKAP5, NCOA5, CASC3, POLD1, PRIM1, TPR, TOPBP1, INCENP
3	4	4	6	PRPF3, DHX16, BUD13, SF3B4
4	3	3	3	SNAPIN, AP3B1, OCRL
5	3	5	6	USP21, UBQLN4, USP14, PTPN23, HGS
6	3	3	3	MED12, MED20, MED24

 $\label{eq:MCODE-molecular} MCODE-molecular complex detection.$

MCODE-Cluster1 was significantly related to the regulation of mRNA processing (Fig. 9).

Therapeutic compound opposing ZNF687

In total, 84 genes were input into CMAP, and the top 3 compounds (amiloride, chaetocin and phloretin) were identified (Table 3). As depicted in Fig. 10, the minimum binding energies of amiloride (PubChem CID: 16231), chaetocin (PubChem CID: 11657687) and phloretin (PubChem CID: 4788) docking ZNF687 protein were correspondingly –5.9 kcal/mol, –8.9 kcal/mol and –6.5 kcal/mol, of which chaetocin exhibited the highest affinity to the ZNF687

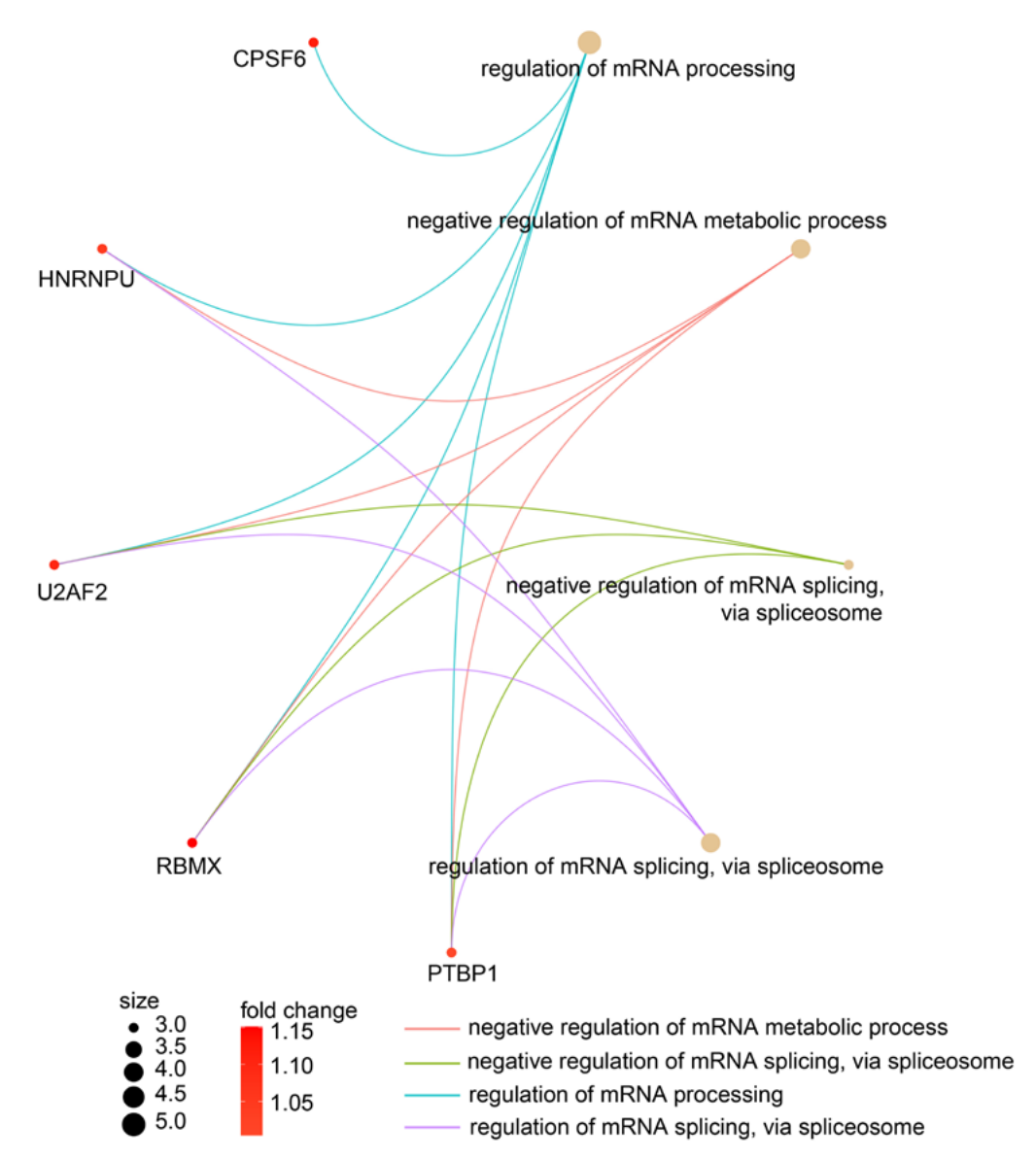


Fig. 9. The Gene Ontology (GO)

– biological process pathway
related to the genes of MCODE-Cluster1

MCODE – molecular complex detection.

protein. The enlarged three-dimensional (3D) structure and the 2D interactions of the binding site are presented in Fig. 10B. Based on the docking result of chaetocin and the ZNF687 protein, the small compound was predicted to form 8 hydrogen bonds with the amino acid residues SER704, ASN705, ALA702, ALA699, GLY701, LEU714, and PRO715, 3 hydrophobic bonds with amino acid residues MET713, PRO698 and LEU695, and an unfavorable acceptor—acceptor interaction with the ANA699 residue.

Discussion

Since 2007, TKI has dramatically improved the treatment of HCC, 29 yet according to a study from 2008, acquired resistance to TKI occurs within 6 months after using TKI drug. 30,31 It is reported that patients with sorafenib resistance had worse OS. 32 Recently, $2^{\rm nd}$ - and $3^{\rm rd}$ -generation TKI have been developed to treat TKI-resistant patients, 33,34 but they are inadequate for overcoming the difficulty of TKI

resistance. The CRISPR screening is a genome-wide editing technology extensively applied in tumor drug-resistance research. CRISPR knockout, CRISPR inhibition and CRISPR activation screens are 3 common methods to explore the drug-resistance mechanism and identify responsible genes.³⁵ In this study, we conducted an in vitro CRISPR knockout screen and confirmed a potential TKI-resistant gene, *ZNF687*. Because *ZNF687* has been reported as overexpressed in HCC, we also collected global cohorts to demonstrate it is an oncogene and is expected to be a druggable target opposing TKI resistance.

In the in vitro study, the gRNA of *ZNF687* was enriched only to a low level, indicating that *ZNF687* knockout likely diminished TKI resistance for HCC cells. This is not the first time a zinc finger protein has been revealed as participating in TKI resistance. In 2020, zinc finger protein 703 was found to induce sorafenib resistance via transactivating CLDN4 expression. However, the underlying mechanism of TKI resistance is unclear, except for presently known processes, including epithelial—mesenchymal

Adv Clin Exp Med. 2025;34(5):787-801

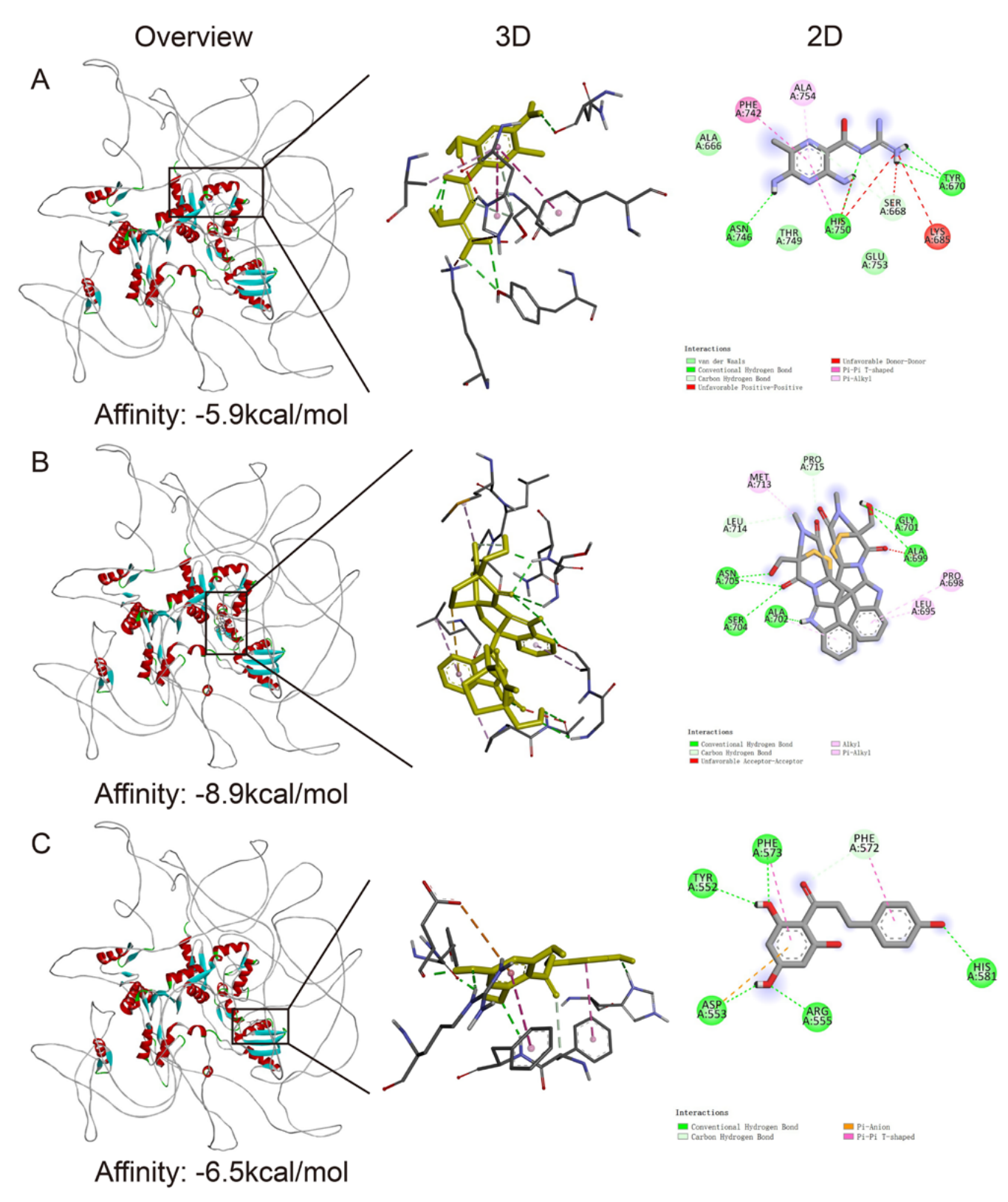


Fig. 10. The overview, enlarged 3D and 2D structures of molecular docking. A. Amiloride and ZNF687; B. Chaetocin and ZNF687; C. Phloretin and ZNF687 Affinity – the binding energy of compound and protein receptor. A lower affinity score indicates the combination is more stable.

transition, ATP-binding cassette transporters, hypoxia, autophagy, and angiogenesis. ¹⁴ Considering that no directly relevant evidence followed, we further explored the potential molecular mechanism of *ZNF687* in HCC.

ZNF687-related differentially expressed genes were enriched for histone modification, nucleocytoplasmic transport, spliceosome, and transcription coregulator activity pathways. Histone modification is essential to resistance,

Table 3. The predicted compounds opposing ZNF687

Compound	Description	Tau	Structure (2D)
Amiloride	sodium channel blocker	-100	H,N-H H,N-H H,N-H H,N-H
Chaetocin	histone lysine methyltransferase inhibitor	-100	H N N N N N N N N N N N N N N N N N N N
Phloretin	sodium/glucose cotransporter inhibitor	-100	H O H

Tau – the connectivity score ranging from –100 to 100. When the connectivity score is closer to 100, the gene list is more similar to the gene perturbation record treated with a compound. Conversely, when the connectivity score is closer to –100, the gene list is more opposite to the gene perturbation record treated with a compound.

with histone modification inhibition, such as histone methylase inhibitors, being demonstrated to reverse tumor drug resistance.³⁷ Additionally, for nucleocytoplasmic transport, it is well known that cancer cells can escape antitumor attacks through the normal nuclear-cytoplasmic transport process or nuclear pore complex. For example, the transport receptor protein CRM1 can mediate drugtarget proteins exported from the nucleus. Consequently, antitumor pharmaceuticals cannot take effect in the nucleus, facilitating resistance.³⁸ Transcriptional coregulator

activity and spliceosome pathways are also implicated in the gene transcription and transcript modification processes. Using the MCODE algorithm and GO enrichment analysis, we showed that *ZNF687*-related differential genes were significantly enriched for the regulation of mRNA processing and splicing. In recent decades, it has been shown that, apart from gene mutations, mRNA alterations are crucial for the occurrence and progression of tumors. Aberrant splicing and polyadenylation of mRNAs are connected with resistance to antitumor therapy, and certain

tumors are highly sensitive to components that inhibit splicing.³⁹ To overcome tumorigenesis and drug resistance caused by abnormal RNA splicing, research on and improvement of splice variant-specific siRNAs, spliceswitching antisense oligonucleotides, and small molecule inhibitors aimed at splicing factors, splicing factor kinases, and aberrant carcinogenic protein isoforms recently been proposed.40 Among the 5 genes found to be participating in the regulation of the mRNA processing pathway in this study, PTBP1, RBMX, HNRNPU, and CPSF6 have been previously shown to enhance HCC development. 41-44 In particular, *RBMX* benefits sorafenib resistance in HCC cells. An obvious reduction in cell viability with increasing sorafenib concentration was observed in RBMX-deficient Huh7/Hch7-SR cells. 42 Moreover, HNRNPU can encourage cisplatin resistance in bladder cancer.45

We performed in silico analysis from tissue and at the cell level and revealed the carcinogenicity of *ZNF687*. Regarding biological functions, zinc finger proteins are involved in transcriptional regulation, protein interactions and post-transcriptional regulation.⁴⁶ Nevertheless, aberrant expression or dysfunction of zinc finger proteins causes hepatocarcinogenesis.^{46,47} For instance, *ZNF687* was previously discovered to promote downstream target gene transcription through binding to the enhancer, thus contributing to HCC.²² Compared with former research, we adopted an increased number of samples and public CRISPR/Cas9 gene-editing data, concluding that *ZNF687* is a prognostic factor for HCC patients and is significant for HCC cell growth.

We determined that *ZNF687* is TKI-resistant and oncogenic, and we subsequently supposed it to be a therapeutic target for overcoming TKI resistance. After further exploration with drug prediction and molecular docking, a small compound chaetocin exhibited a potential to resist ZNF687 in this study. Chaetocin is a natural metabolite from *Chaetomium* and has been reported to have an antitumor effect on various malignancies, including HCC.^{48,49} Notably, chaetocin was previously claimed to overcome TKI resistance for chronic myelogenous leukemia.⁵⁰ Consequently, we propose that chaetocin can oppose TKI resistance to HCC through targeting ZNF687.

The highlights of the present study include the execution of in vitro CRISPR screening to identify the TKI-resistant gene *ZNF687*, integrated global sequencing datasets and public CRISPR/Cas9 knockout data to attest its carcinogenicity, and implemented a molecular simulation to declare ZNF687 a druggable target. We comprehensively illuminated the possible functions of *ZNF687* and the biological mechanism. The underlying molecular mechanism of *ZNF687* may be related to histone modification, spliceosome, transcription coregulator activity, and nucleocytoplasmic transport.

Limitations

During the collection of mRNA datasets of HCC tissue and calculating the demonstrated transcriptional expression status of the *ZNF687* gene, the authors detected high heterogeneity. However, random-effects analysis was adopted to make up for the deficiency. Conversely, the biological pathways that *ZNF687* may be involved in were predicted in this study, but they have not been verified through in vivo or in vitro experiments. Thus, robust experimental verification should be conducted for an intensive understanding of *ZNF687*.

Conclusions

ZNF687 was shown to be a TKI-resistant and growth-dependent gene for HCC, and overexpression of *ZNF687* indicates poor OS for HCC patients. Additionally, ZNF687 is expected to be a druggable target for overcoming TKI resistance, and chaetocin may be a candidate therapeutic compound for ZNF687.

Supplementary data

The Supplementary materials are available at https://doi.org/10.5281/zenodo.11075935. The package includes the following files:

Supplementary Table 1. Gene effects of zinc finger protein 687 deletion on the growth of hepatocellular carcinoma cell lines.

Supplementary Table 2. Statistical description and the true positive, false positive, true negative and false negative values of zinc finger protein 687 mRNA in datasets.

Supplementary Table 3. Exploring the sources of high heterogeneity using univariable meta-regression analysis Supplementary Fig. 1. Sensitivity analysis using the one-by-one removal method.

Supplementary Fig. 2. Proportional hazards assumption test by Schoenfeld residual method. A. *ZNF687*-continuous (p = 0.16); B. Age (p = 0.97); C. Gender (p = 0.15); D. Race (p < 0.05); E. pT stage (p = 0.66); F. AJCC stage (p = 0.53). Supplementary Fig. 3. Log-linear hypothesis test by Martingale residual method.

Data availability

The datasets generated and/or analyzed during the current study are available from the corresponding author on reasonable request.

Consent for publication

Not applicable.

ORCID iDs

Guan-Lan Zhang Dhttps://orcid.org/0009-0003-4825-5555

Jian-Di Li Dhttps://orcid.org/0000-0001-7050-371X

Ji-Feng He Dhttps://orcid.org/0009-0002-8382-5376

Kun-Jun Wu Dhttps://orcid.org/0000-0002-1492-4533

Ying-Yu Mo Dhttps://orcid.org/0009-0003-4207-0584

Song-Yang Zhong Dhttps://orcid.org/0009-0009-5902-7527

Xuan-Fei Wang Dhttps://orcid.org/0009-0009-649-4916

Yi-Si Qin Dhttps://orcid.org/0009-0003-0733-1451

Hong Zhao Dhttps://orcid.org/0009-0003-0543-2689

Zhi-Guang Huang Dhttps://orcid.org/0000-0003-4457-9491

Gang Chen Dhttps://orcid.org/0000-0003-2402-2987

Rong-Quan He Dhttps://orcid.org/0000-0002-7752-2080

References

- Siegel RL, Miller KD, Wagle NS, Jemal A. Cancer statistics, 2023. CA Cancer J Clin. 2023;73(1):17–48. doi:10.3322/caac.21763
- Sung H, Ferlay J, Siegel RL, et al. Global cancer statistics 2020: GLO-BOCAN estimates of incidence and mortality worldwide for 36 cancers in 185 countries. CA Cancer J Clin. 2021;71(3):209–249. doi:10.3322/caac.21660
- Shen C, Jiang X, Li M, Luo Y. Hepatitis virus and hepatocellular carcinoma: Recent advances. *Cancers (Basel)*. 2023;15(2):533. doi:10.3390/cancers15020533
- 4. Huang M, Liu J, Fan Y, et al. Development of curcumin-loaded galactosylated chitosan-coated nanoparticles for targeted delivery of hepatocellular carcinoma. *Int J Biol Macromol*. 2023;253:127219. doi:10.1016 /j.ijbiomac.2023.127219
- Köckerling F, Sheen AJ, Berrevoet F, et al. The reality of general surgery training and increased complexity of abdominal wall hernia surgery. Hernia. 2019;23(6):1081–1091. doi:10.1007/s10029-019-02062-z
- Işık A, Fırat D. Letter to the editor concerning "Most cited 100 articles from Turkey on abdominal wall hernias: A bibliometric study." Turk J Surg. 2021;37(2):193–194. doi:10.47717/turkjsurg.2021.4973
- Woo HY, Han SY, Heo J, et al. Role of endoscopic biliary drainage in advanced hepatocellular carcinoma with jaundice. PLoS One. 2017; 12(11):e0187469. doi:10.1371/journal.pone.0187469
- Isik A, Poyanli A, Tekant Y, et al. Incomplete or inappropriate endoscopic and radiologic interventions as leading causes of cholangitis. Pol Przegl Chir. 2021;93(6):47–52. doi:10.5604/01.3001.0015.0423
- Chakraborty E, Sarkar D. Emerging therapies for hepatocellular carcinoma (HCC). Cancers (Basel). 2022;14(11):2798. doi:10.3390/cancers 14112798
- Roskoski R. Properties of FDA-approved small molecule protein kinase inhibitors: A 2023 update. *Pharmacol Res.* 2023;187:106552. doi:10.1016/j.phrs.2022.106552
- 11. Xing R, Gao J, Cui Q, Wang Q. Strategies to improve the antitumor effect of immunotherapy for hepatocellular carcinoma. *Front Immunol*. 2021;12:783236. doi:10.3389/fimmu.2021.783236
- Wang D, Zheng X, Fu B, et al. Hepatectomy promotes recurrence of liver cancer by enhancing IL-11-STAT3 signaling. eBioMedicine. 2019;46:119–132. doi:10.1016/j.ebiom.2019.07.058
- Man KF, Ma S. Mechanisms of resistance to tyrosine kinase inhibitors in liver cancer stem cells and potential therapeutic approaches. Essays Biochem. 2022;66(4):371–386. doi:10.1042/EBC20220001
- Tian Y, Lei Y, Fu Y, Sun H, Wang J, Xia F. Molecular mechanisms of resistance to tyrosine kinase inhibitors associated with hepatocellular carcinoma. Curr Cancer Drug Targets. 2022;22(6):454–462. doi:10.2174/1568009622666220330151725
- Ma Y, Zhang L, Huang X. Genome modification by CRISPR/Cas9. FEBS J. 2014;281(23):5186–5193. doi:10.1111/febs.13110
- Lander ES. The heroes of CRISPR. Cell. 2016;164(1–2):18–28. doi:10.1016 /j.cell.2015.12.041
- Jinek M, Chylinski K, Fonfara I, Hauer M, Doudna JA, Charpentier E. A programmable dual-RNA-guided DNA endonuclease in adaptive bacterial immunity. *Science*. 2012;337(6096):816–821. doi:10.1126/science.1225829
- Zhang F, Wen Y, Guo X. CRISPR/Cas9 for genome editing: Progress, implications and challenges. Hum Mol Genet. 2014;23(R1):R40–R46. doi:10.1093/hmg/ddu125

- Shalem O, Sanjana NE, Hartenian E, et al. Genome-scale CRISPR-Cas9 knockout screening in human cells. Science. 2014;343(6166):84–87. doi:10.1126/science.1247005
- Burton HW, Carlson BM, Faulkner JA. Microcirculatory adaptation to skeletal muscle transplantation. *Annu Rev Physiol*. 1987;49(1): 439–451. doi:10.1146/annurev.ph.49.030187.002255
- 21. Divisato G, Formicola D, Esposito T, et al. ZNF687 mutations in severe Paget disease of bone associated with giant cell tumor. *Am J Hum Genet*. 2016;98(2):275–286. doi:10.1016/j.ajhg.2015.12.016
- Zhang T, Huang Y, Liu W, et al. Overexpression of zinc finger protein 687 enhances tumorigenic capability and promotes recurrence of hepatocellular carcinoma. *Oncogenesis*. 2017;6(7):e363. doi:10.1038/oncsis.2017.63
- Gennari L, Rendina D, Falchetti A, Merlotti D. Paget's disease of bone. Calcif Tissue Int. 2019;104(5):483–500. doi:10.1007/s00223-019-00522-3
- 24. Scotto Di Carlo F, Whyte MP, Gianfrancesco F. The two faces of giant cell tumor of bone. *Cancer Lett.* 2020;489:1–8. doi:10.1016/j.canlet. 2020.05.031
- Joung J, Konermann S, Gootenberg JS, et al. Genome-scale CRISPR-Cas9 knockout and transcriptional activation screening. *Nat Protoc*. 2017;12(4):828–863. doi:10.1038/nprot.2017.016
- 26. Iversen GR, Gergen MM. Statistics: The Conceptual Approach. New York, USA: Springer; 1997. ISBN:978-0-387-94610-8
- Subramanian A, Narayan R, Corsello SM, et al. A next generation connectivity map: L1000 platform and the first 1,000,000 profiles. *Cell*. 2017;171(6):1437–1452.e17. doi:10.1016/j.cell.2017.10.049
- Trott O, Olson AJ. AutoDock Vina: Improving the speed and accuracy of docking with a new scoring function, efficient optimization, and multithreading. J Comput Chem. 2010;31(2):455–461. doi:10.1002/jcc.21334
- Llovet JM, Ricci S, Mazzaferro V, et al. Sorafenib in advanced hepatocellular carcinoma. N Engl J Med. 2008;359(4):378–390. doi:10.1056/ NEJMoa0708857
- 30. Sui Z, Xue H, Jing F, Leng P. Sorafenib plus capecitabine for patients with advanced hepatocellular carcinoma. *China Pharmacy.* 2008; (11):848–849 [in Chinese].
- Tang W, Chen Z, Zhang W, et al. The mechanisms of sorafenib resistance in hepatocellular carcinoma: Theoretical basis and therapeutic aspects. Sig Transduct Target Ther. 2020;5(1):87. doi:10.1038/s41392-020-0187-x
- 32. Ogasawara S, Chiba T, Ooka Y, et al. Post-progression survival in patients with advanced hepatocellular carcinoma resistant to sorafenib. *Invest New Drugs*. 2016;34(2):255–260. doi:10.1007/s10637-016-0323-1
- Han Z, He Z, Wang C, Wang Q. The effect of apatinib in the treatment of sorafenib resistant metastatic hepatocellular carcinoma: A case report. *Medicine (Baltimore)*. 2018;97(49):e13388. doi:10.1097/MD.000000000013388
- Tan CS, Kumarakulasinghe NB, Huang YQ, et al. Third generation EGFR TKIs: Current data and future directions. *Mol Cancer*. 2018;17(1):29. doi:10.1186/s12943-018-0778-0
- 35. Alyateem G, Wade HM, Bickert AA, et al. Use of CRISPR-based screens to identify mechanisms of chemotherapy resistance. *Cancer Gene Ther.* 2023;30(8):1043–1050. doi:10.1038/s41417-023-00608-z
- Wang H, Xu H, Ma F, et al. Zinc finger protein 703 induces EMT and sorafenib resistance in hepatocellular carcinoma by transactivating CLDN4 expression. *Cell Death Dis*. 2020;11(4):225. doi:10.1038/s41419-020-2422-3
- Yang C, Zhang J, Ma Y, Wu C, Cui W, Wang L. Histone methyltransferase and drug resistance in cancers. J Exp Clin Cancer Res. 2020; 39(1):173. doi:10.1186/s13046-020-01682-z
- 38. Turner JG, Dawson J, Sullivan DM. Nuclear export of proteins and drug resistance in cancer. *Biochem Pharmacol.* 2012;83(8):1021–1032. doi:10.1016/j.bcp.2011.12.016
- Desterro J, Bak-Gordon P, Carmo-Fonseca M. Targeting mRNA processing as an anticancer strategy. Nat Rev Drug Discov. 2020;19(2):112–129. doi:10.1038/s41573-019-0042-3
- 40. Wang BD, Lee N. Aberrant RNA splicing in cancer and drug resistance. *Cancers (Basel)*. 2018;10(11):458. doi:10.3390/cancers10110458
- 41. Kang H, Heo S, Shin JJ, et al. A miR-194/PTBP1/CCND3 axis regulates tumor growth in human hepatocellular carcinoma. *J Pathol*. 2019;249(3):395–408. doi:10.1002/path.5325

- Song Y, He S, Ma X, et al. RBMX contributes to hepatocellular carcinoma progression and sorafenib resistance by specifically binding and stabilizing BLACAT1. Am J Cancer Res. 2020;10(11):3644–3665. PMID:33294259. PMCID:PMC7716158.
- 43. Liang Y, Fan Y, Liu Y, Fan H. HNRNPU promotes the progression of hepatocellular carcinoma by enhancing CDK2 transcription. *Exp Cell Res.* 2021;409(1):112898. doi:10.1016/j.yexcr.2021.112898
- 44. Tan S, Zhang M, Shi X, et al. CPSF6 links alternative polyadenylation to metabolism adaption in hepatocellular carcinoma progression. *J Exp Clin Cancer Res*. 2021;40(1):85. doi:10.1186/s13046-021-01884-z
- 45. Shi ZD, Hao L, Han XX, et al. Targeting HNRNPU to overcome cisplatin resistance in bladder cancer. *Mol Cancer*. 2022;21(1):37. doi:10.1186/s12943-022-01517-9
- 46. Li X, Han M, Zhang H, et al. Structures and biological functions of zinc finger proteins and their roles in hepatocellular carcinoma. *Biomark Res.* 2022;10(1):2. doi:10.1186/s40364-021-00345-1

- 47. Li Q, Tan G, Wu F. The functions and roles of C2H2 zinc finger proteins in hepatocellular carcinoma. *Front Physiol.* 2023;14:1129889. doi:10.3389/fphys.2023.1129889
- 48. Zhang Q, Ruan F, Yang M, Wen Q. Natural compound chaetocin induced DNA damage and apoptosis through reactive oxygen species-dependent pathways in A549 lung cancer cells and in vitro evaluations. *IET Nanobiotechnol*. 2023;17(5):465–475. doi:10.1049/nbt2.12144
- 49. Hu P, Hu L, Chen Y, et al. Chaetocochin J exhibits anti-hepatocellular carcinoma effect independent of hypoxia. *Bioorg Chem.* 2023;139: 106701. doi:10.1016/j.bioorg.2023.106701
- 50. Truitt L, Hutchinson C, DeCoteau JF, Geyer CR. Chaetocin antileukemia activity against chronic myelogenous leukemia cells is potentiated by bone marrow stromal factors and overcomes innate imatinib resistance. *Oncogenesis*. 2014;3(10):e122. doi:10.1038/oncsis.2014.37